Desalination 503 (2021) 114951

Contents lists available at ScienceDirect

Desalination

journal homepage: www.elsevier.com/locate/desal

Approximation of dynamic membrane distillation processes applied to concentration of aqueous sucrose solutions

Martijn Bindels [a,b,*], Bart Medaer [a,b], Mekonnen Gebrehiwot [b], Bart Nelemans [a]

[a] Aquastill, Nusterweg 69, 6136 KT Sittard, the Netherlands
[b] Faculty of Engineering Technology, Campus Group T Leuven, KU Leuven, Leuven, Vesaliusstraat 13, 3000, Belgium

HIGHLIGHTS

- A methodology is presented to approximate dynamic processes of vacuum assisted air gap membrane distillation (V-AGMD).
- A setup for the validation was designed and used.
- The resulting approximation fits the experimental data well.
- An approximation for treating aqueous sucrose solutions is presented.
- The first module with an oleophobic and hydrophobic membrane is presented.
- A Brix concentration of 56.9 was reached in a semi batch process.

GRAPHICAL ABSTRACT

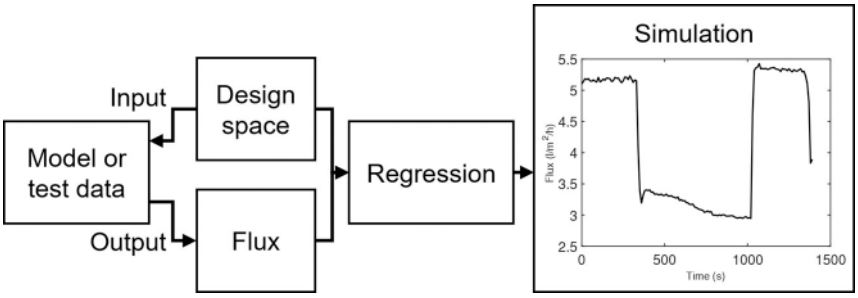

ARTICLE INFO

Keywords:
Modelling
Vacuum assisted air gap membrane distillation (V-AGMD)
Oleophobic coating
Solar desalination
Sucrose

ABSTRACT

In this work, a method is presented for the approximation of dynamic processes. Dynamic inputs of membrane distillation can be approximated by a regression equation as several steady state steps after each other. A regression equation of the flux was developed based on a validated steady state model and a wide range of process parameters. The regression equation of the flux is then used to approximate a dynamic process. To test the approximation on a dynamic process, a new test setup was developed to provide quick changes to the temperatures or flow. It was found that the approximation corresponds well to the test results. While this paper only approximates the flux, the method presented in this paper can also be used to approximate other variables. The presented method is also applied to the concentration of aqueous sucrose solutions with an AGMD module with oleophobic and hydrophobic properties. Three semi batch tests were done. The approximation corresponds well to the test results. A maximum Brix concentration of 56.9 was reached in the tests.

1. Introduction

The ongoing population growth and climate change cause a challenge to provide clean drinking water worldwide. Currently, around two billion people face water stress, and this number is expected to increase [1]. A possible solution which is gaining momentum is membrane distillation (MD). MD uses a vapour pressure difference coming from two streams with a temperature difference across a semipermeable hydrophobic membrane. Due to its hydrophobicity, only water vapour can pass through the membrane. This way, one side of the membrane is in

* Corresponding author at: Aquastill, Nusterweg 69, 6136 KT Sittard, the Netherlands.
E-mail address: m.bindels@aquastill.nl (M. Bindels).

https://doi.org/10.1016/j.desal.2021.114951
Received 27 September 2020; Received in revised form 22 December 2020; Accepted 7 January 2021
Available online 22 January 2021

contact with the feed water while the other side of the membrane is in contact with the distillate. Several setups for MD have been investigated. In Direct Contact Membrane Distillation (DCMD), the hot feed water and the cold distillate is in direct contact with the membrane [2]. In Air Gap Membrane Distillation (AGMD), an air gap is placed in between the hot and cold feed to reduce the conduction losses [3]. In Vacuum-Assisted Air Gap Membrane Distillation (V-AGMD), the air gap is placed under a partial vacuum, V-AGMD is better performing than AGMD [4].

MD can be used with a wide variety of green energy sources. For example, it can be used in combination with solar [5–11], solar ponds [12–14], wind energy [15], and geothermal energy [16]. However, the mentioned energy sources have a variable thermal energy output, which results in dynamic behaviour of the hot feed side, and consequently, in a dynamic distillate output. Still, there are only few models concerning the dynamic calculation of the distillate output [17–23]. In the work of Chang et al. [17] a dynamic model was developed for a solar driven membrane distillation desalination system (SMDDS). The model included the spiral-wound air gap membrane distillation (SP-AGMD) module, the heat exchanger, solar collector, and heat storage tank.

Emad ali performed dynamic analysis and modelling of direct contact membrane distillation (DCMD) [18]. His work complemented the work of Eleiwi et al. [19] and Karam et al. [20]. Eleiwi et al. [19] proposed a model for direct contact membrane distillation (DCMD) which was based on a 2D Avection-Diffusion Equation (ADE). Karam et al. [20] made a model for DCMD based on a lumped-parameter dynamic predictive model. The model used the analogy of electrical system for heat and mass transfer problems. Porrazzo et al. [21] a neural network model of a MD system powered by solar energy was developed. Emad ali et al. [22] also developed a linear dynamic model during start up of DCMD, the reaction curve method was used for the identification of the model. In another work of Emad ali et al. [23] evaluated lumped parameter and special dynamic models.

Another way of simulating dynamic process is by approximation several points along the process instead of simulating the total dynamic process. There are several benefits of using approximations instead of a full dynamic model. The benefits are as follows:

- The solutions of (partial) differential equations are not needed. This reduces the complexity of the solution and reduces the computation time.
- Multiple sources of data can be used. A steady state or dynamic model is not needed as the approximation can also be done with test data. If test data is used, it removes the modelling error of the model.
- No specialized software needed. The approximation can be done with Matlab but can also be done with Excel. Even more, the result of the approximation can also be used with pen and paper calculations.
- As steady state data can be used, no dynamic validation is needed. Steady state validation can be done with limited apparatus while for dynamic validation more expensive setup is needed.
- The modelling along the complete dynamic process is not needed. Several points along the process can be calculated and interpolation can be used to approximate the process between the calculated points.
- The control hardware of a system can be cheaper and smaller as the equations for approximation are less demanding compared to the DAE models.

In this work, an approximation is developed for dynamic processes of MD based on a previously developed steady state model [24]. The benefit is that there exists a wide range of steady state models [2,24–29]. In Fig. 1, the proposed methodology of developing the approximation is shown.

The validated steady state model is used to generate data over a wide range of input parameters, such as crossflow velocity, salinity, air gap pressure for V-AGMD setup, membrane and condenser inlet temperatures. To increase the efficiency of the methodology, the data points are not chosen randomly but within a design space. The steady state AGMD model described and validated in [24], is then used to generate the output data, which is the flux. However, the proposed method can also be used for the approximation of gained output ratio (GOR), or other output parameters of a model. Furthermore, this methodology can also be applied with test data, as long as it is sufficient to provide a reasonable regression equation. The data points and the output of the steady state model at those points are then used to create a regression formula that can be used to approximate the dynamic processes. It should be noted that the proposed methodology can also be used with other equations obtained with experimental data. For example, the experimentally determined equations from Ruiz Aguirre et al. [10] can also be used for the approximation. The dynamic process can be approximated as several steady state steps that follow the dynamic profile of the inputs,

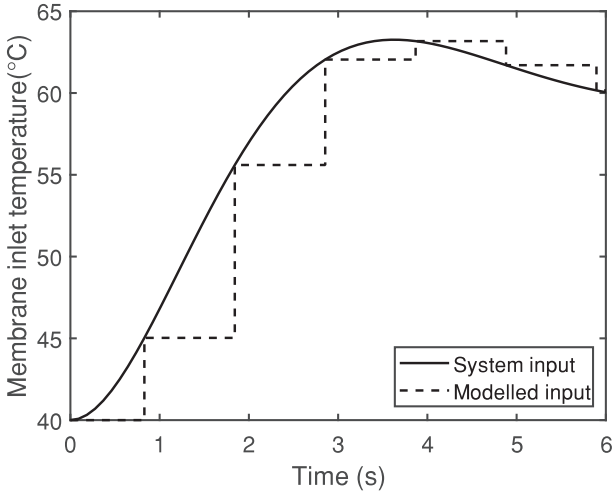

Fig. 2. Modelling dynamic inputs with steady state steps. The dynamic inputs are modelled by several steady state steps.

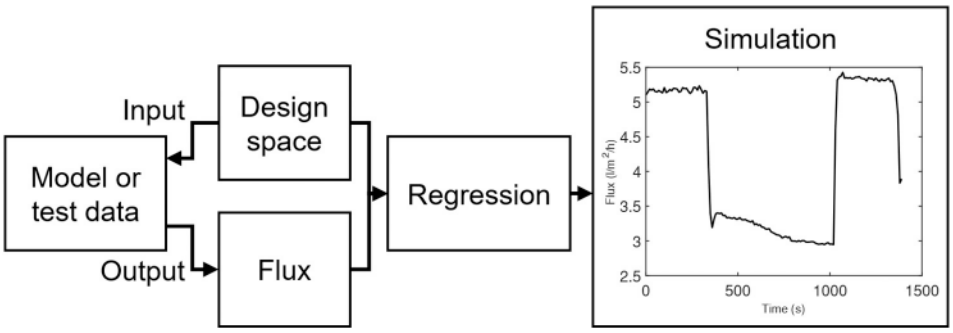

Fig. 1. Method for determining the approximation.

as will be proven later in this work. A schematic view can be seen in Fig. 2. The use of steady state steps assumes that the transient effects of the membrane distillation module are negligible, as long as the time between the steady state steps are small enough.

To prove that the approximation works, it was employed on the concentration of aqueous sucrose with an AGMD module with a hydrophobic and oleophobic membrane. The validated steady state model is fed with the thermophysical properties of sucrose solutions so that the model can be applied to sucrose solutions. Then the methodology that is presented in this paper is applied to generate an approximation for dynamic processes. The approximation formula is then used to simulate the three semi batch tests.

2. Theoretical background

2.1. Space-filling designs

Two general methods can be used to gather the data needed for creating a regression formula. The first one is by doing physical experiments and the second one is by running a computer simulation. Computer simulations are often used when physical experiments are time or resource intensive. However, a computer model should be available to acquire the necessary test results. In addition, the computer simulation should represent the real system accurately, otherwise, the results may be inaccurate [30,31].

The experiments that are calculated in computer simulation are often based on a design space that is created to make sure that there is a design point close to any point in the experimental region [31]. Several space-filling designs were developed in the past, such as the minimax distance, the maximin distance and Latin hypercube design methods. In minimax distance design, the smallest distance will be maximized between any two points in the design space [32]. The downside of this method is the possibility of good space-filling for a single dimension while projections in other dimensions may not be sufficient [31]. In maximin distance design, the largest distance will be minimized between any two points in the design space [32]. This method has the same downside as the minimax method. A sufficient projection may exist in one dimension, but not in the other dimensions [31]. In Latin hypercube design, the design space is divided into $n2$ squares, where n is the number of points. Afterwards, the points are randomly placed in one of the squares. The only constraint is that only one point can be placed in every row and column, while the benefit of this method is better projecting for two dimensions. However, in higher dimensions poor projection is still possible. The second problem is the possibility that the points align diagonally [31].

To overcome that the points align diagonally, maximin Latin hypercube design was developed. This method works with the same principle as normal Latin hypercube design except an extra constraint is added. The extra constraint forces the points to be as far from other points as possible, and as a result, there is only a poor projection in high dimensions [31].

In the maximum projection method, the poor projection in higher dimension is solved. In this method, a weighted Euclidean distance function is used so that the projection is sufficient in every dimension. Thus, the maximum projection method is the best overall method [33]. The statistical program R [34] with the Maxpro package [35] will be used to create the design space in this paper.

2.2. Steady state model

A previously developed steady state model from Aquastill [24] was used in this work. However, the method presented in this work can also be used with other steady state models. To use the steady state model from [24] for V-AGMD the pressure used for the calculation of the membrane permeability should be the pressure in the air gap.

To convert the model to aqueous sucrose solutions, the thermophysical properties of Table 1 were used in the steady state model. Not all the equations found are valid for the range of temperatures where MD operates. For example, the density is valid from 10 to 60 °C. Therefore, a possible error might occur due to the extrapolation of these equations.

2.3. Second order multiple regression model

For the approximation, a second order multiple regression equation is used. In Eq. (1), the standard second-order multiple regression model can be seen. Since a first-order model will not be able to fit perfect for quadratic relationships between different variables, the second-order model was chosen for designing the regression model. In eq. (1) β_i with $i = 0, 1, \ldots, k$ are the regression coefficients and x_i with $i = 0, 1, \ldots, k$ are the variables that are called the predictor variables or regressors [41].

$$y = \beta_0 + \beta_1 x_1 + \beta_2 x_2 + \ldots + \beta_k x_k + \beta_{11} x_1^2 + \beta_{22} x_2^2 + \ldots + \beta_{kk} x_k^2 + \beta_{12} x_1 x_2 + \beta_{13} x_1 x_3 + \ldots + \beta_{1k} x_1 x_k + \beta_{23} x_2 x_3 + \beta_{24} x_2 x_4 + \ldots + \beta_{2k} x_2 x_k + \ldots \beta_{k-1,k} x_{k-1} x_k \quad (1)$$

In Table 2, the predictor variables are listed. In total five variables can change during operation of V-AGMD. A slightly wider range than practically expected were chosen for the membrane inlet and condenser inlet to be sure that the regression formula still performs well near the boundaries of the variables.

2.3.1. Regression coefficients

According to Myers et al. [41], the least squares method is the most used method for finding the regression coefficients, and will be used in this work. In Eq. 2 the formula for finding the different regression coefficients can be seen. More information on the derivation of the formula can be found in [41]. The matrix $\boldsymbol{b}$ represents all the regression coefficients. The matrix $\boldsymbol{X}$ is called the model matrix, and it consists in the created experimental points from the design space. The matrix $\boldsymbol{y}$ contains the results that were obtained from the model.

$$\boldsymbol{b} = (\boldsymbol{X}'\boldsymbol{X})^{-1}\boldsymbol{X}'\boldsymbol{y} \quad (2)$$

2.3.2. Model adequacy checking

Adequacy checking should be done to make sure that the regression formula corresponds to the physical system. There are several methods for checking the model adequacy. Some common methods are actual versus prediction plot, residual analysis, scaling residuals, influence diagnostics and testing for lack of fit. More information about these methods can be found in [41]. In this work checking model adequacy will be done with an actual versus prediction plot and residual analysis as this is an effective method [42].

In Fig. 3, a possible actual versus prediction plot is shown. In this plot, the results of regression formula are plotted in function of the simulated response. The straight line in the plot represents a perfect fit between regression and the data. In other words, when all the points align, the regression formula (y_{reg}) represents the simulation results (y_{sim}) perfectly [41]. The actual versus prediction plot will only give a good indication if the regression formula represents the simulation results. Therefore, a more advanced method like residual analysis is

Table 1
Equations used to convert the NaCl model to sucrose solutions.

Type	Reference
Water activity	[36]
Density	[37]
Specific heat	[38]
Viscosity	[39]
Thermal conductivity	[40]

Table 2
Predictor variables and the chosen limits.

Predictor variables	Minimum value	Maximum value	Symbol
Condenser inlet temperature (°C)	15	35	$T_{cond,\ in}$
Membrane inlet temperature (°C)	65	90	$T_{mem,\ in}$
Salinity (g/kg)	0	200	S
Air gap pressure (*kPa*)	10	100	P_{airgap}
Cross flow velocity (m/s)	0.03	0.15	v_{eff}

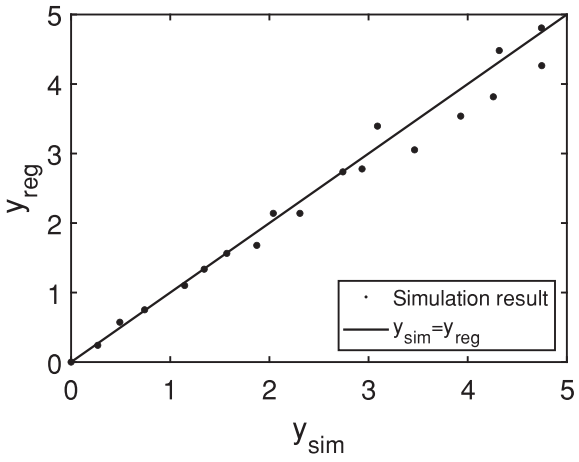

Fig. 3. Example of an actual versus prediction plot. The y_{reg} corresponds to the results obtained based on the regression equation while y_{sim} represents the actual test data or simulation data.

needed.

The residual analysis consists of two parts. In the first part, a normal probability plot of the residuals is constructed, which is capable of checking the normality assumption in a simple way [42]. In this plot, the residuals are plotted against the normal probability, an example of can be seen on the left in Fig. 4. On the right of Fig. 4, possible residuals in function of the predicted response are shown, which gives more information about the variance of the response.

2.4. Regression-based approximation

When assuming that the transient effects are neglectable, a regression formula can be used to model the system. The time-varying system, Eq. (3), can be discretized to Eq. (4). The total distillate production can then be approximated with Eq. (5), where T_d and A_m are the discretization time (the time between to steady state steps) and the membrane area, respectively. The same process can be done for the heat input, which is shown by Eq. (6). Eqs. (4) and (6) can then be combined to produce the GOR, which is shown in Eq. (7).

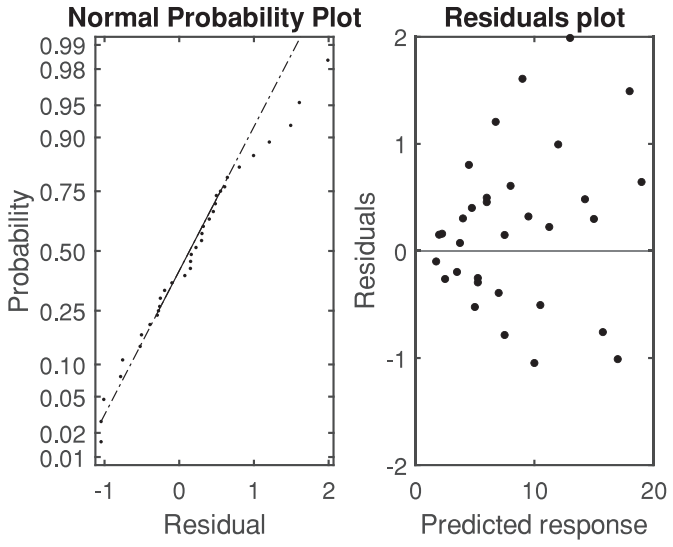

Fig. 4. Normal probability plot and Residual plot.

$$J(t) = f\left(T_{con,in}(t)\ ,T_{mem,in}(t)\ ,S_{in}(t)\ ,v_{eff}(t)\ ,P_{air\ gap}(t)\right) \tag{3}$$

$$J[k] = f\left(T_{con,in}[k]\ ,T_{mem,in}[k]\ ,v_{eff}[k]\ ,S_{in}[k]\ ,P_{air\ gap}[k]\right) \tag{4}$$

$$D_{tot} = A_m T_d \sum_{1}^{n} J_i \tag{5}$$

$$Q_{in}[k] = f\left(T_{con,in}[k]\ ,T_{mem,in}[k]\ ,v_{eff}[k]\ ,S_{in}[k]\ ,P_{air\ gap}[k]\right) \tag{6}$$

$$GOR[k] = \frac{H_v J[k] A_m T_d}{Q_{in}[k]} \tag{7}$$

$T_{con,\ in}$, $T_{mem,\ in}$, S_{in}, v_{eff} and $P_{air\ gap}$ are the condenser and membrane inlet temperatures, inlet salinity, effective velocity, and air gap pressure, respectively. D_{tot} is the total distillate output and J is the flux in l/m^2/h and T_d is the time between discretisation steps in hours. v_{eff} can be also be changed to the feed flow.

3. Materials and methods

Two types of test have been employed in this work. The first type of test consists of step functions to validate the approximation models of V-AGMD with NaCl solutions. The second type of test are three semibatch tests to prove that the methodology works.

3.1. V-AGMD and NaCl tests

The approximation should be validated for steady state and dynamic tests. The source for the steady state data comes from [24] where an AGMD module with a membrane area of 7.2 m2 from Aquastill was used. As most systems are designed for steady state operation it is usually not possible to apply a step input to validate the dynamics of the approximation eq. A typical steady state setup is shown in Fig. 5. To apply a step input of the temperatures, salinity, or flow, two pilots were interconnected, which resulted in Figs. 6 and 7. For this work, an AGMD module with a membrane area of 7.2 m2 was used, with a slightly thinner airgap than in [24] to improve the drainage of the distillate from the air gap. The specifications of the module used in this work can be found in Tables 3 to 6.

As can be seen in Fig. 6, the membrane and condenser streams from the two pilots are connected to the AGMD module by using four instead of two tanks. Therefore, it is possible to have two membrane and two condenser inlet water temperatures. To switch between the two tanks, valves are placed in front of the entries of the module. This way, it is possible to perform a step input. A bypass valve was used to make sure that the feed flow from both pilots is the same. The hot feed water tanks were heated by electrical heaters. The cold feed tanks were cooled by a heat exchanger with water cooling. The distillate produced by the module is collected in a 30-l tank and weighted on a scale. In Table 7, all the used measuring equipment are listed. In Fig. 7 the real setup is shown.

To have a measurable response, the magnitude of the step input should be significant. To see the effect of the magnitude several step magnitudes were chosen. All the input charts can be seen in Appendix A, and are summarized in Table 8. The pressure in the air gap and the cold feed temperature is kept constant as this does not change quickly in real applications.

Valves were used to apply a step input. The valves where placed

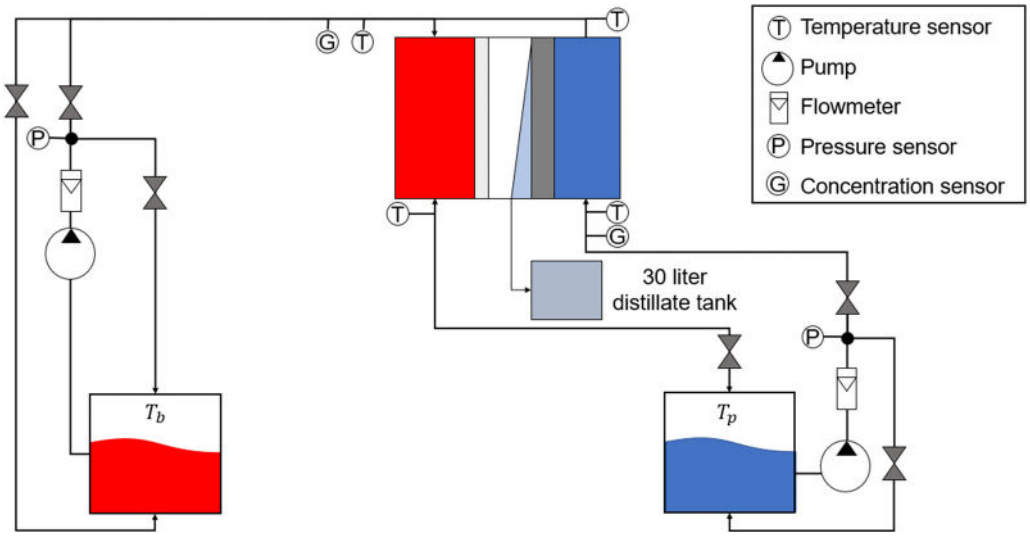

Fig. 5. Schematic representation of a steady state test setup. In this case a combi pilot is shown.

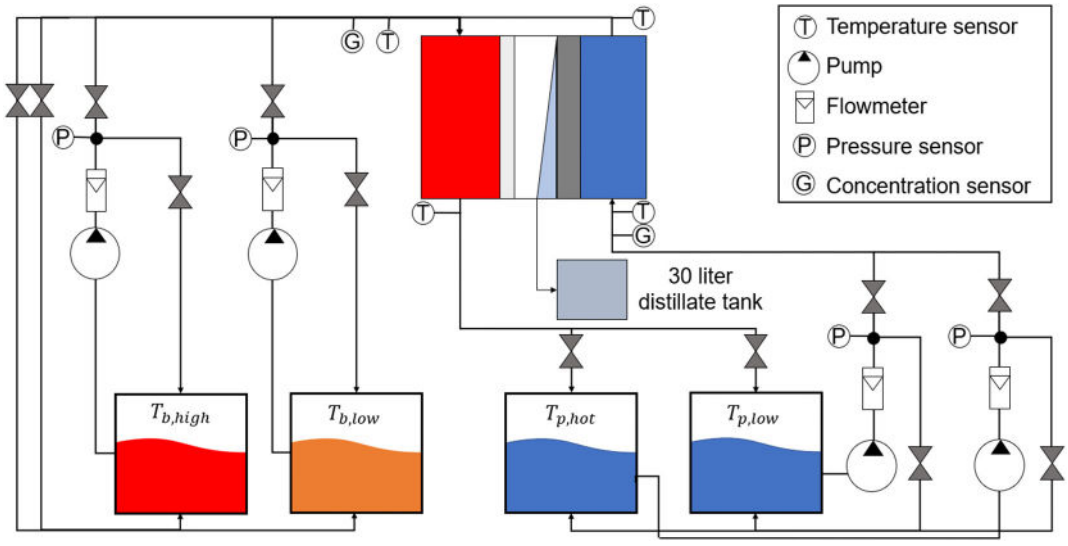

Fig. 6. Schematic representation of the dynamic test setup.

before the module entries and after the module exit, on both the condenser and membrane side. A bypass was used to make sure that the pilots could run continuously even when the valves to the module were closed.

3.2. AGMD and semi batch sucrose tests

A new AGMD module was developed with a membrane with oleophobic and hydrophobic properties which has better wetting prevention than a normal hydrophobic membrane. The same membrane as normal modules are used, but with the application of the oleophobic coating. The spacer channels are the same as for the V-AGMD unit. However, the air gap channel is slightly different. The air gap channel thickness and porosity are 0.845 mm and 88.7% for the AGMD sucrose module, respectively.

For the semi batch tests the same setup as in [24] was used but with a better weight balance and a smaller tank. The sucrose concentration was measured with the HI96800 refractometer from Hanna instruments. The sugar was bought from a local supermarket. According to the label, an anticaking agent was added to the sucrose. The test conditions can be seen in Table 9. The temperatures and flows were kept constant during the test.

The start volume or mass is needed to simulate the concentration rise during the test. The volume in the tank can be measured by using distance meters and using geometry to identify the total volume in the tank. As the tank is not uniform in shape this can give inaccurate results. Therefore, the following equation was used to calculate the starting mass of water in the tank:

$$m_0 = \frac{C_{end} D_{tot}}{C_{end} - C_{start}} \tag{8}$$

where C_{end}, C_{start}, and D_{tot} are the concentration at the end, start concentration, and the total produced distillate. This equation works with the assumption that the produced distillate is pure water. This is not always the case, but the amount of sucrose in the distillate is negligibly small. Therefore, this equation gives a better estimation than measuring it with a distance meter and geometry.

Fig. 7. Actual setup used in this work. Module can be seen in the middle, with the valves on top and at the bottom of the outlet and inlet. On the left and the right, the two individual pilots can be seen.

Table 3
Module specifications.

Module specifications (AS7)	Value
Channel or envelope height	0.4 m
Channel or envelope length	1.5 m
Number of channels or envelopes	6
Total membrane area	7.2m^2

Table 4
Membrane and condenser channel specifications.

Membrane and condenser channel parameters	Value
Spacer channel thickness	2.01 mm
Number of spacer strands	240
Spacer angle	60°
Spacer filament length	4.17 mm

Table 5
Air gap specifications.

Air gap parameters	Value
Spacer thickness	0.81 mm
Spacer angle	90°
Spacer filament length	3.33 mm

Table 6
Membrane specifications.

Membrane specifications	Value
Membrane pore size	$1.6 \cdot 10^{-7} m$
Membrane porosity	0.85
Membrane thickness	$9.5 \cdot 10^{-5} m$

Table 7
Measurement equipment used in this work.

Measurement	Type
Flow	Burkert 8041 and Burkert 8020
Salinity	Burkert 8228
Temperature	Burkert Pt-100
Balance	Vida xl A4-LCD

Table 8
Dynamic change in each test.

Test	Dynamic change	Low value	High value	Type of change
1	Membrane inlet	75 °C	79 °C	Slow ramp
2	Membrane inlet	45 °C	80 °C	Step
3	Flow, Crossflow velocity	550 l/h, 0.0405 m/s	1000 l/h, 0.0737 m/s	Step
4	Flow, Crossflow velocity	375 l/h, 0.0276 m/s	650 l/h, 0.0479 m/s	Step
5	Membrane inlet	70 °C	80 °C	Step
6	Membrane inlet	60 °C	80 °C	Step
7	Salinity	Tap water	35 g/kg	Block
	Membrane inlet	80 °C	65 °C	Step

The salinity could not be measured experimentally because the value was out of range of the sensors. Therefore, the salinity was calculated based on the amount of water in the tank and the amount of salt that was added to the tank.

4. Results and discussion

4.1. V-AGMD model for NaCl

4.1.1. Regression model

In total, 400 simulations were run as this was found to give adequate results. The approximation equation was obtained from the regression for the flux in $l/m^2/h$:

Table 9
Test conditions of the sucrose batch test with AGMD. The reported membrane inlet, condenser inlet, and the flow are the average value during the test.

Semi batch test	Start concentration (°Brix)	End concentration (°Brix)	Membrane inlet (°C)	Condenser inlet (°C)	Flow or crossflow velocity (l/h), (m/s)
1	6.875	29.375	70.8	23.3	830, 0.0612
2	7.325	34.4	70.7	23.4	830, 0.0612
3	23.4	56.933	70.6	24.5	830, 0.0612

$$J = a_0 + a_1 T_{con} + a_2 T_{mem} + a_3 S_{NaCl} + a_4 P_a + a_5 Q_f + a_6 T_{con}^2 + a_7 T_{mem}^2 + a_8 S_{NaCl}^2 + a_9 P_a^2 + a_{10} Q_f^2 + a_{11} T_{con} T_{mem} + a_{12} T_{con} S_{NaCl} + a_{13} T_{con} P_a + a_{14} T_{con} Q_f + a_{15} T_{mem} S_{NaCl} + a_{16} T_{mem} P_a + a_{17} T_{mem} Q_f + a_{18} S_{NaCl} P_a + a_{19} S_{NaCl} Q_f + a_{20} P_a Q_f \quad (9)$$

where T_{con}, T_{mem}, S_{NaCl}, P_a, Q_f are the condenser and membrane inlet temperatures in °C, salinity in g/kg, air gap pressure in Pa, and feed flow in m^3/h, respectively. The regression coefficients can be found in Table 10. Note that the equation is only valid for an AS7 module.

4.1.2. Model adequacy

The actual versus residual plot is shown on the left side of Fig. 8. Almost all points align perfectly with the line, thus, the regression formula may be a good representation of the simulation results. However, since some points deviate from the line, a residual analysis is needed to make sure that the equation is acceptable.

The normal probability plots can be seen on the right side of Fig. 8. The shape of the normal probability plot indicates that there is a heavy-tailed distribution [42]. The residual plot can be seen in Fig. 9, and shows, that the residuals are high for low and high fluxes.

4.1.3. State space model

The approximation model can be written as a discrete state space model:

$$x[k+1] = Ax[k] + Bu[k] \quad (10)$$

$$y[k] = Cx[k] + Du[k] \quad (11)$$

By using fictitious states x_1 and x_2, which represents the flux and the total distillate production, the following state space model can be developed. The state space equation also contains fictitious input that corresponds to the higher terms in the regression equation. The state space equation is as follows:

$$\begin{bmatrix} x_{1,k+1} \\ x_{2,k+1} \end{bmatrix} = \begin{bmatrix} 0 & 0 \\ T_d A_m & 1 \end{bmatrix} \begin{bmatrix} x_{1,k} \\ x_{2,k} \end{bmatrix} + \begin{bmatrix} a_0 & a_1 & \dots & a_5 & a_6 & \dots & a_{10} & a_{11} & \dots & a_{20} \\ 0 & 0 & \dots & 0 & 0 & \dots & 0 & 0 & \dots & 0 \end{bmatrix} \begin{bmatrix} 1 \\ T_{con} \\ \vdots \\ Q_f \\ T_{con}^2 \\ \vdots \\ Q_f^2 \\ T_{con} T_{mem} \\ \vdots \\ P_a Q_f \end{bmatrix} \quad (12)$$

$$\begin{bmatrix} J_k \\ D_k \end{bmatrix} = \begin{bmatrix} 1 & 0 \\ 0 & 1 \end{bmatrix} \begin{bmatrix} x_{1,k} \\ x_{2,k} \end{bmatrix} + 0 \cdot u[k] \quad (13)$$

where T_d and A_m are the time between steps in hours and the membrane area in m^2, respectively. The state space equation can be used for control purposes.

4.1.4. Steady state validation

As can be seen in Fig. 10, the approximation and the test result for the flux correspond well with the model from [24], with an error below

Table 10
Regression coefficients of the regression formula. *E*-b stands for 10^{-b}, so E-5 stands for 10^{-5}.

Coefficient	Value	Coefficient	Value	Coefficient	Value
a_0	6.441 E-1	a_7	4.152 E-4	a_{14}	−6.863 E-2
a_1	2.464 E-2	a_8	−2.167 E-5	a_{15}	−2.369 E-4
a_2	−2.811 E-2	a_9	5.435 E-11	a_{16}	−1.972 E-7
a_3	1.176 E-2	a_{10}	−7.539 E-1	a_{17}	1.524 E-1
a_4	−5.098 E-6	a_{11}	−1.436 E-4	a_{18}	3.563 E-8
a_5	−1.298	a_{12}	6.190 E-5	a_{19}	−6.407 E-3
a_6	−1.290 E-3	a_{13}	5.665 E-7	a_{20}	−1.856 E-5

10%.

4.1.5. Dynamic validation

Due to using two interconnected pilots the flow of the hot and cold brine are slightly different from each other (around 25 l/h). Therefore, for the regression equation, the mean flow was used to approximate the flux.

The time between the approximation points was taken as 10 s ($T_d = \frac{10}{3600}$ as T_d is expressed in hours), which was the same as the sample time of the test. As can be seen in Figs. 13 and 14, the regression follows the test results closely. However, at the end of test 1, the regression follows the test result less closely. The reason for this is that the air gap can act as a water reservoir that can empty suddenly. This happens at the end of test 1, which results in a higher flux than expected. This also happened in the other direction, where no distillate came out of the module, this is observed in test 4. Test 1 and 4 are shown in Figs. 11 and 12. Nevertheless, in general, approximation followed the production closely, as can be seen in Figs. 13 and 14.

For test 3, shown in Fig. 15, at 1100 s into the test, the total production was measured wrong resulting in a negative flux which is not possible and was, therefore, left out of the data. Despite this, the approximation underestimates the test results only with a small error.

In test 5, which is shown in Fig. 16, the approximation slightly overestimates the distillate production. Therefore, the overshooting (like in test 5) might compensate for the undershooting (like in test 3) in a practical application. The same can be seen in the results of test 2 (overestimation of the approximation) and test 6 (underestimation of the approximation).

The test result with the salt shock can be seen in Fig. 17. The earlier described emptying of the air gap can again be seen in this test twice. Once around 400 s and around 1000 s. Overall, the approximation still closely matches the results.

As can be seen in Fig. 18, the time between the steps (T_d) can be changed to a higher value without loss of accuracy. However, higher than 90 s (or $T_d = \frac{90}{3600}$ h) is not advised as this increases the error of the approximation. At first, a lowering of the time between the steps

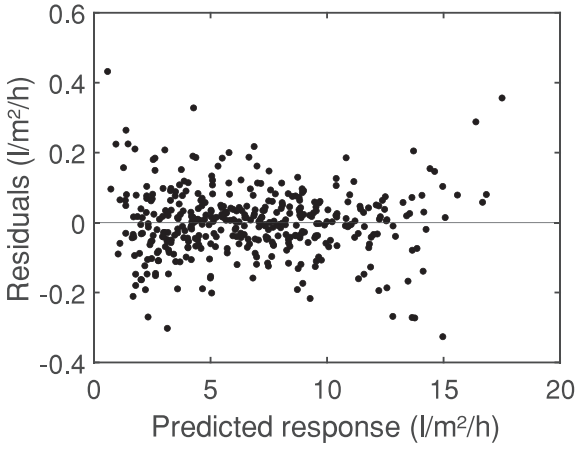

Fig. 9. Residual plot of the flux.

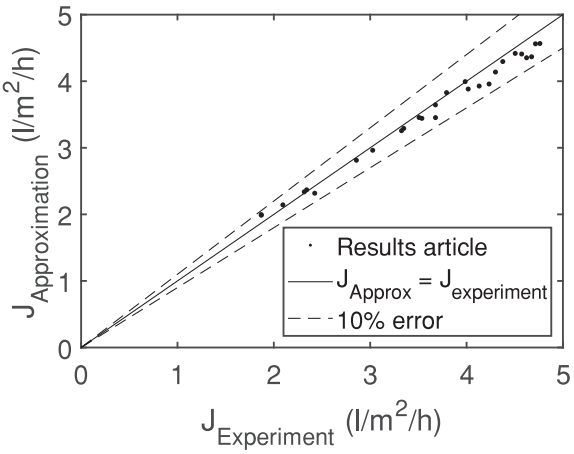

Fig. 10. Predicted flux versus measured flux of the regression model. The article results are from [24]. Approx stands for approximation.

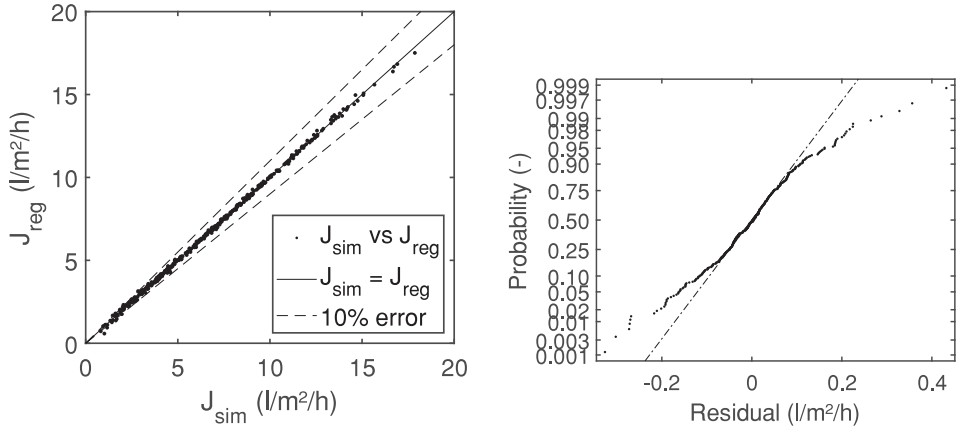

Fig. 8. Actual versus prediction plot (left) and normal probability plot (right).

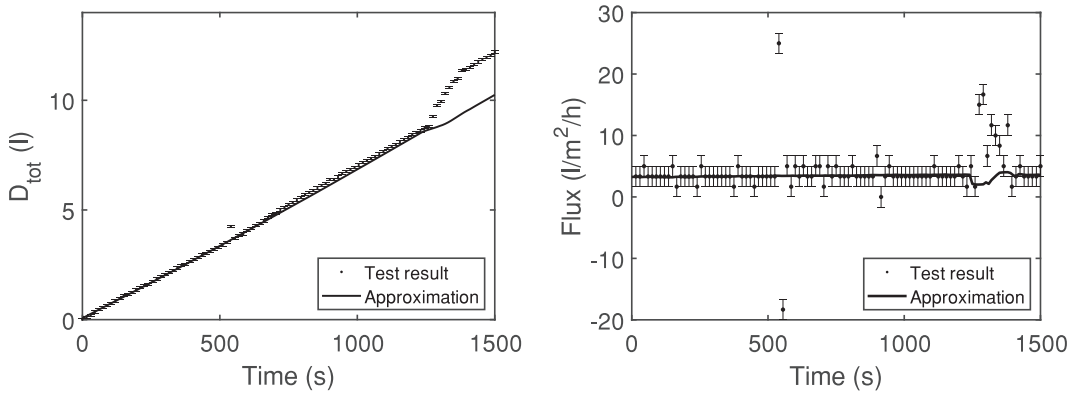

Fig. 11. Test result of test 1. On the left the total production. On the right the flux.

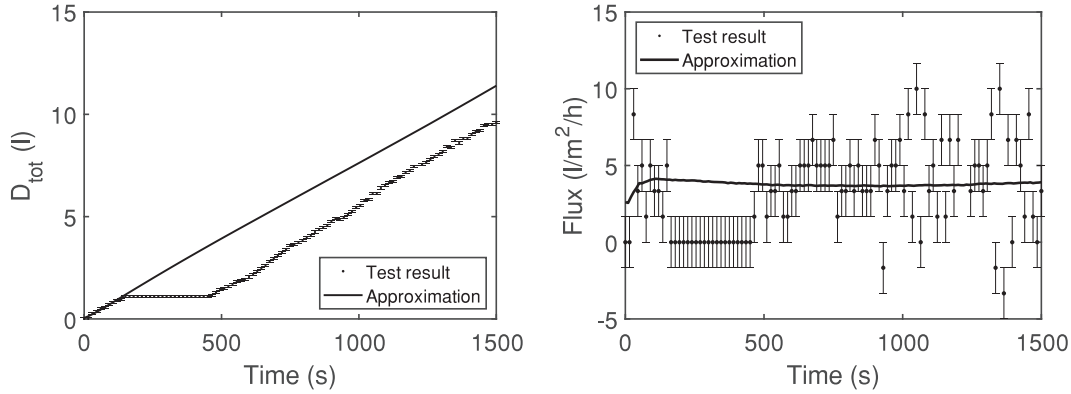

Fig. 12. Test result of test 4. On the left the total production. On the right the flux.

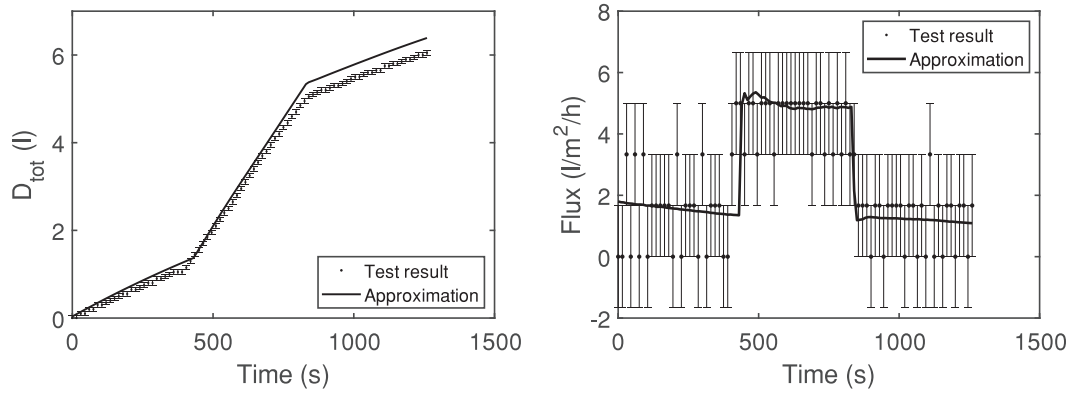

Fig. 13. Test result of test 2. On the left the total production. On the right the flux.

reduced the error. This is due to the time discrepancy between the measurement of the temperatures and the measurement of the amount of distillate. The temperatures are measured directly in the pipe, while the distillate first must travel out of the module before it enters the distillate tank where it is weighed. This result in a delay between the time that the distillate is produced versus the time of measurement. Therefore, the results with a longer time between steps are more accurate.

The step response is the fastest response the system can have. Therefore, it can be stated that all dynamic processes can be approximated with a time between steps of 90 s, or $T_d = \frac{90}{3600}$h.

4.2. AGMD and sucrose model

4.2.1. Regression model

As previously, 400 simulations were run as this was found to give adequate results. The following equation was obtained from the regression for the flux in $l/m^2/h$:

$$J = a_0 + a_1 T_{con} + a_2 T_{mem} + a_3 Brix + a_4 Q_f + a_5 T_{con}^2 + a_6 T_{mem}^2 + a_7 Brix^2 + a_8 Q_f^2 + a_9 T_{con} T_{mem} + a_{10} T_{con} Brix + a_{11} T_{con} Q_f + a_{12} T_{mem} Brix + a_{13} T_{mem} Q_f + a_{14} Brix Q_f \quad (14)$$

where T_{con}, T_{mem}, $Brix$, and Q_f are the condenser and membrane inlet temperature in °C, sucrose concentration in degree Brix, and feed flow in

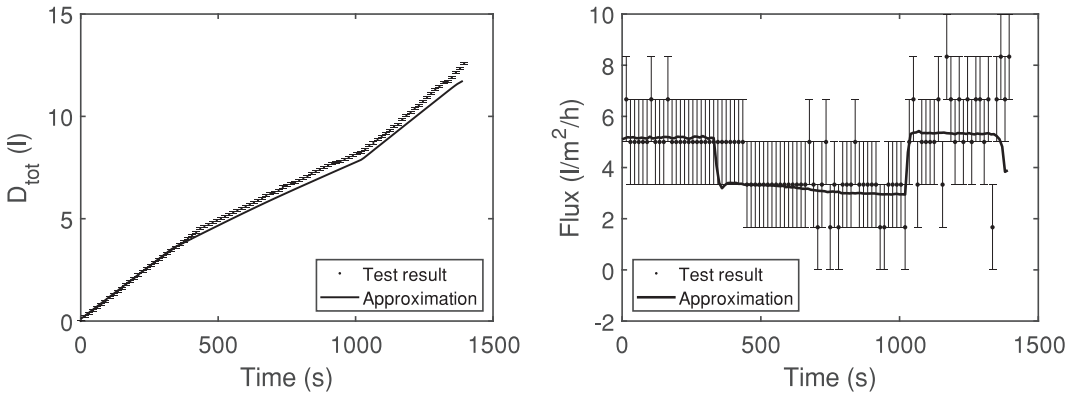

Fig. 14. Test result of the test 6. On the left the total production. On the right the flux.

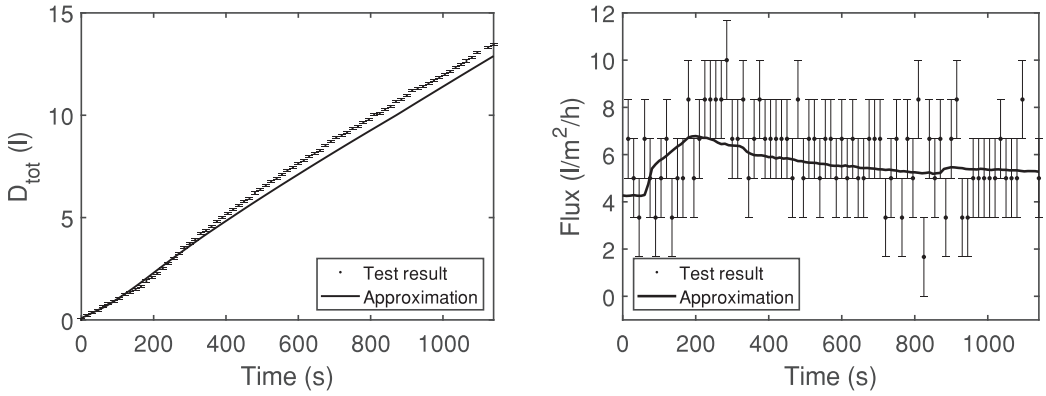

Fig. 15. Test result of test 3. On the left the total production. On the right the flux.

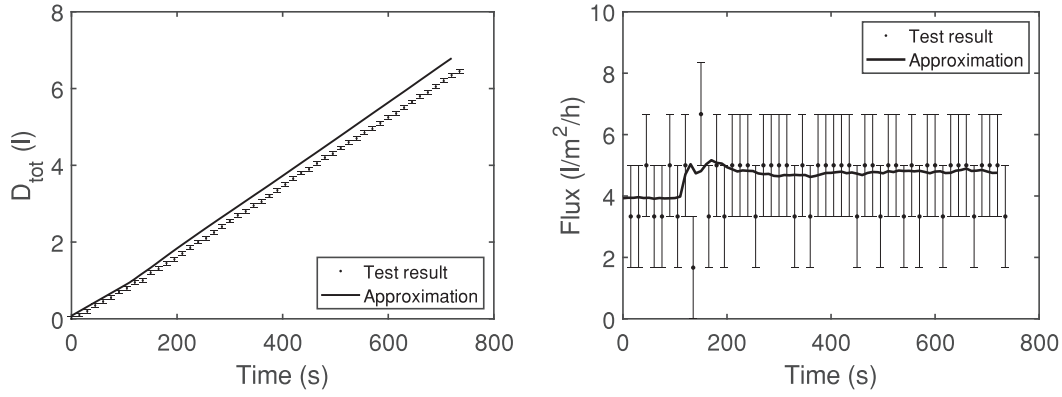

Fig. 16. Test result of test 5. On the left the total production. On the right the flux.

m^3/h, respectively. The regression coefficients can be found in Table 11. Note that the equation is only valid for an AS7 module, which is specified in previous sections.

4.2.2. Model adequacy

The actual versus residual plot is shown on the left side of Fig. 8. The points in this plot represent the simulated results in function of the predicted results of the regression model. Almost all points align perfectly with the line, thus, the regression formula may be a good representation of the simulation results. However, since some points deviate from the line, a residual analysis is needed to make sure that the equation is acceptable.

The normal probability plots can be seen on the right side of Fig. 19. As for the V-AGMD model of NaCl solution, the shape of the normal probability plot indicates that there is a heavy-tailed distribution [42]. The residual plot can be seen in Fig. 20, and indicates that the approximation works better for higher fluxes (>5 $l/m^2/h$) than for lower fluxes (<5 $l/m^2/h$).

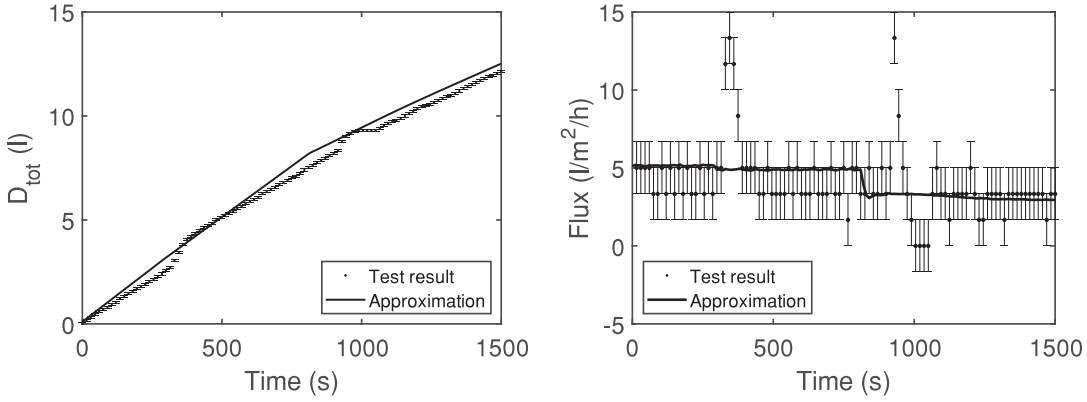

Fig. 17. Test result of test 7. On the left the total production. On the right the flux.

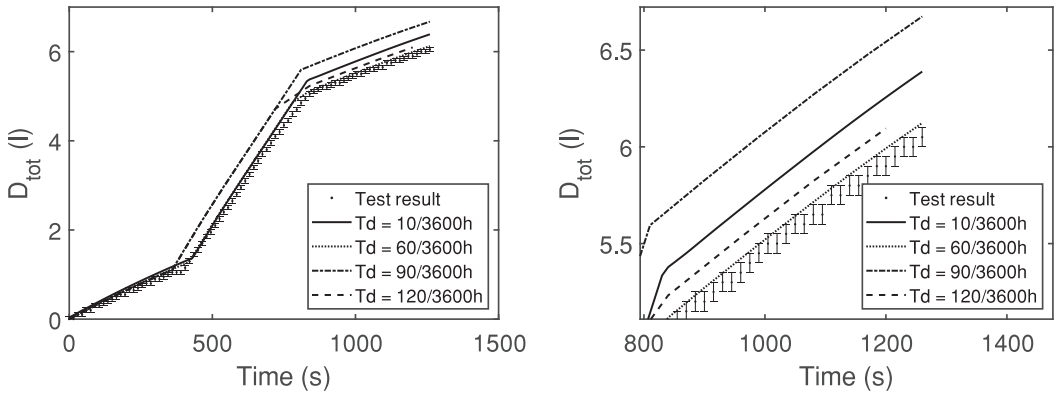

Fig. 18. Results of test 4 with different Td. The results at the end of the test are shown in more detail on the right.

Table 11
Regression coefficients of the regression formula. *E*-b stands for 10^{-b}, so E-5 stands for 10^{-5}.

Coefficient	Value	Coefficient	Value	Coefficient	Value
a_0	−0.2334	a_5	−0.00107	a_{10}	2.9536 E-4
a_1	0.0466	a_6	4.192 E-4	a_{11}	−0.0481
a_2	−0.0237	a_7	1.6072 E-5	a_{12}	−7.1481 E-4
a_3	0.0377	a_8	−0.6807	a_{13}	0.1205
a_4	−1.6241	a_9	−1.9657 E-4	a_{14}	−0.0176

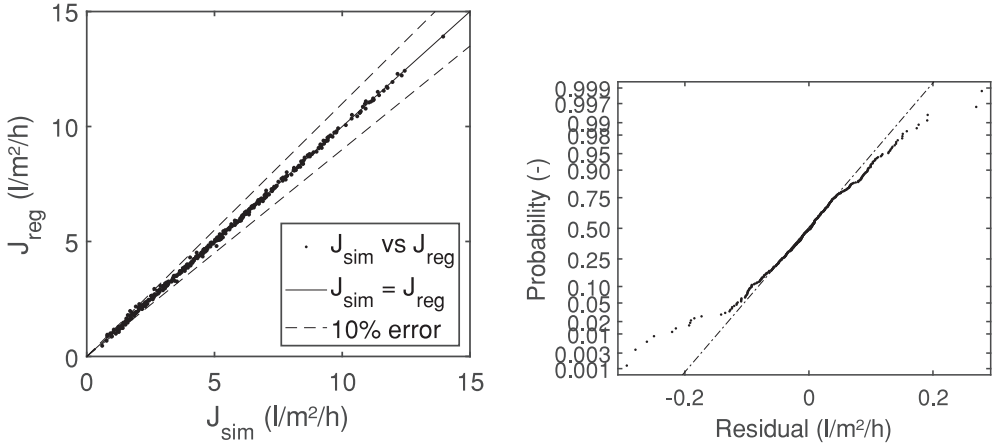

Fig. 19. Actual versus prediction plot (left) and normal probability plot (right) of the AGMD sucrose model.

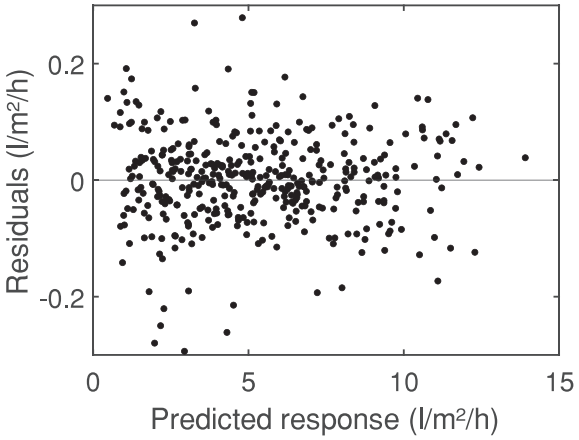

Fig. 20. Residual plot of the flux for the sucrose AGMD approximation.

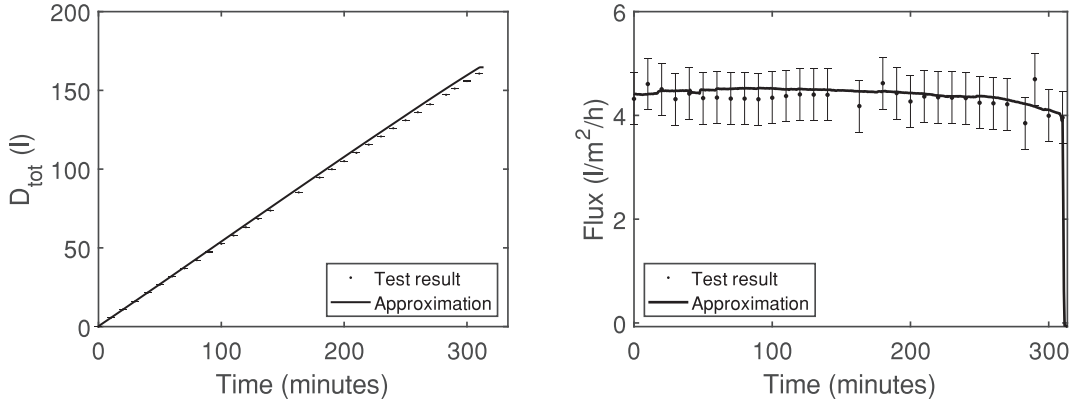

Fig. 21. Test result of semi batch test 1. On the left the total production. On the right the flux.

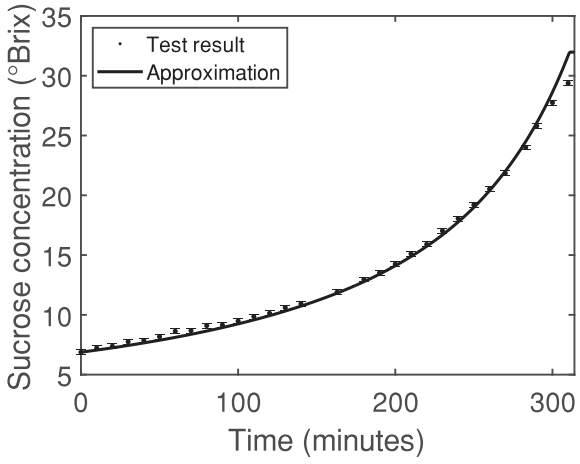

Fig. 22. Approximated versus test results of the concentration during the test of semi batch test 1.

4.2.3. Dynamic validation

The test results for the semi batch test can be seen in Figs. 21 to 26. The approximation match the test results closely for the flux and the total distillate production. At the end of the test, the approximated flux goes to zero as the first two tests were run till the tank was almost empty, and the pumps could not work anymore. Therefore, the pumps were stopped which cause the feed flow to go to zero. For the third test, the maximum pressure of the module was reached, and the test was stopped prematurely to prevent module damage. Consequently, a measurement of the flux was made before stopping the test and the stopping of the pump is not shown in the graph. All the approximations were done with 30 s between approximations, ($T_d = \frac{30}{3600}$ as T_d is expressed in hours).

The approximated sucrose concentration at the end is slightly higher than the measured results. A possible reason for this is the slight overestimation of flux during the approximation which results in more removed distillate and thus, in a higher end concentration. Another possible reason is that it is assumed in the approximation that the removed distillate is pure water. However, there might still be some sucrose in the distillate and thus less sucrose left in the feed tank. Overall, it can be concluded that the proposed methodology can be used to approximate dynamic process over a wide range of applications.

5. Conclusion

When using green energy to generate heat for membrane distillation the provided water temperatures are generally not constant. Hence, an approximation is developed to calculate the flux with non-constant inputs. The dynamic input can be approximated as several steady state inputs as long as the time difference between the two steps is smaller than 90 s. To test the dynamic behaviour a new test setup was developed. In standard setups, the temperatures and flows could not be changed fast enough. In this work, two test setups were interconnected to form one test setup where the input can be changed rapidly. The approximation equation closely corresponds to the test results, even though in some test it slightly overestimates and in other it slightly

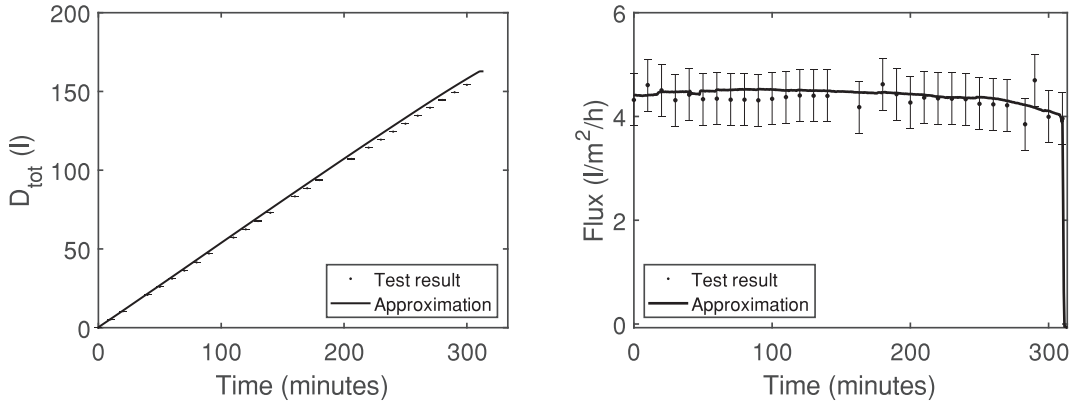

Fig. 23. Test result of semi batch test 2. On the left the total production. On the right the flux.

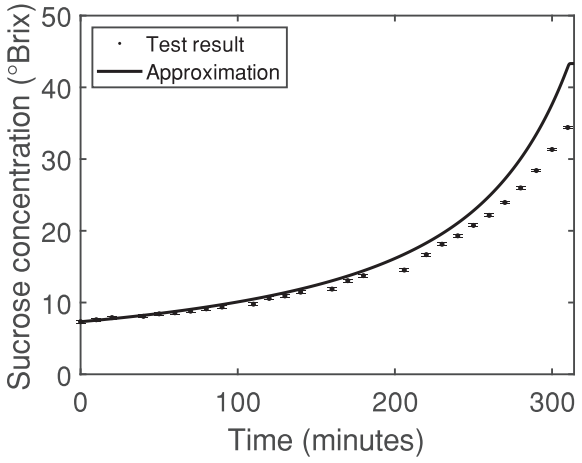

Fig. 24. Approximated versus test results of the concentration during the test of semi batch test 2.

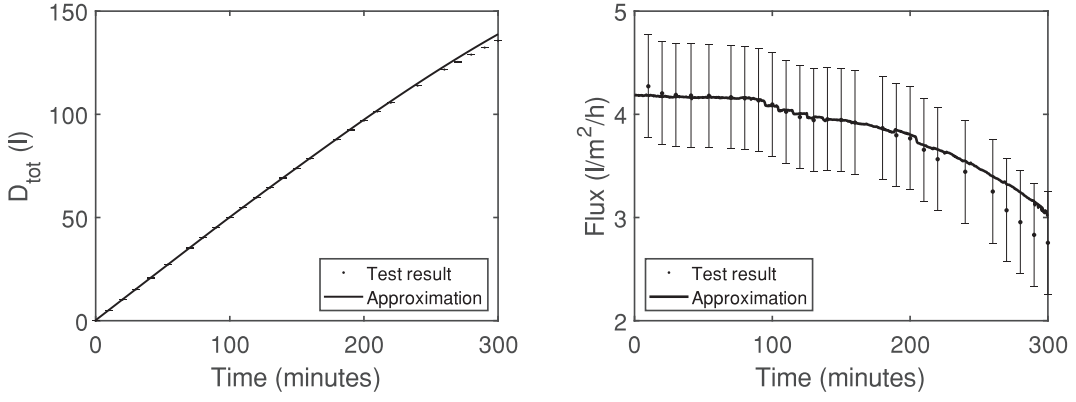

Fig. 25. Test result of semi batch test 3. On the left the total production. On the right the flux.

underestimates the test results. In practice, the over and underestimation would be less noticeable as the overestimation and underestimation null each other out over a long time. It was also found that the air gap can act as a reservoir that holds the water or releases the water suddenly, which can result in a sudden increase or decrease in distillate production, causing an overestimation or underestimation of the test results.

To prove that the methodology works, three semi batch tests on an aqueous sucrose solution were performed. The approximation matches the test results of the flux and the total distillate production closely. However, there is a deviation between the approximated sucrose concentration and the tested concentration. This might be due to overestimation of the flux of approximation or due to small traces of sucrose in the distillate. In the end, it can be concluded that the proposed methodology can be used for the approximating dynamic processes.

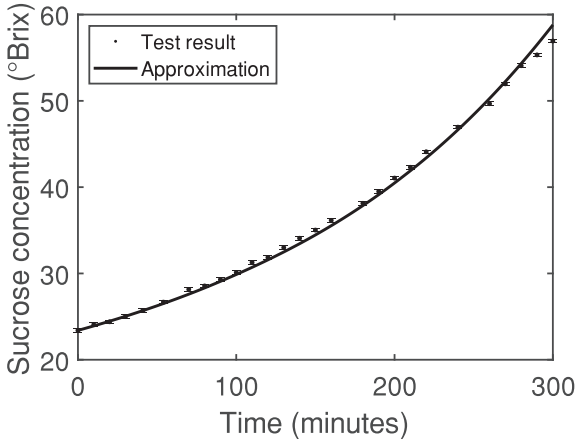

Fig. 26. Approximated versus test results of the concentration during the test of semi batch test 3.

CRediT authorship contribution statement

Martijn Bindels: Conceptualization, Methodology, Software, Validation, Formal analysis, Investigation, Data Curation, Writing-Original Draft, Writing- Review and Editing, Visualization

Bart Medaer: Conceptualization, Methodology, Software, Validation, Formal analysis, Investigation, Data Curation, Writing-Original Draft, Writing- Review and Editing, Visualization

Mekonnen Gebrehiwot: Supervision, Project administration

Bart Nelemans: Resources, Supervision, Project administration, Funding acquisition

Declaration of competing interest

The authors declare that they have no known competing financial interests or personal relationships that could have appeared to influence the work reported in this paper.

Appendix A. Dynamic test conditions

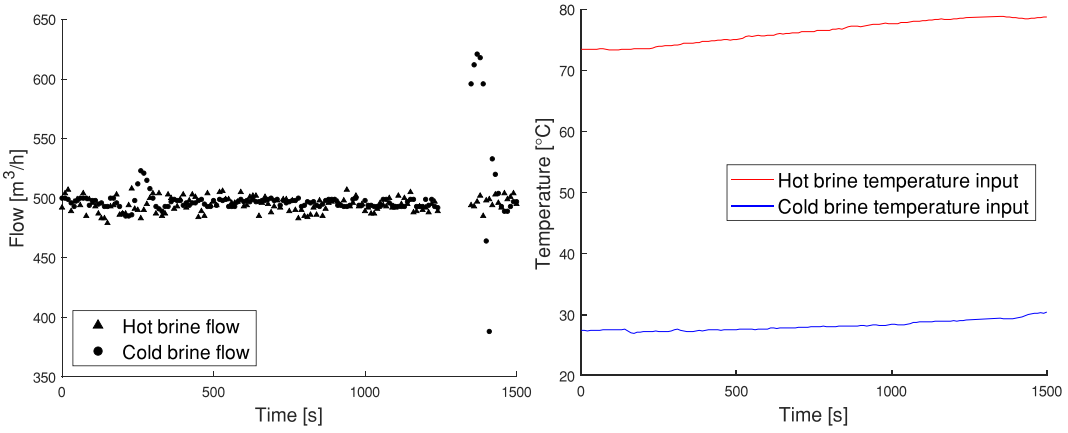

Fig. A1. Test flow and temperatures of test 1.

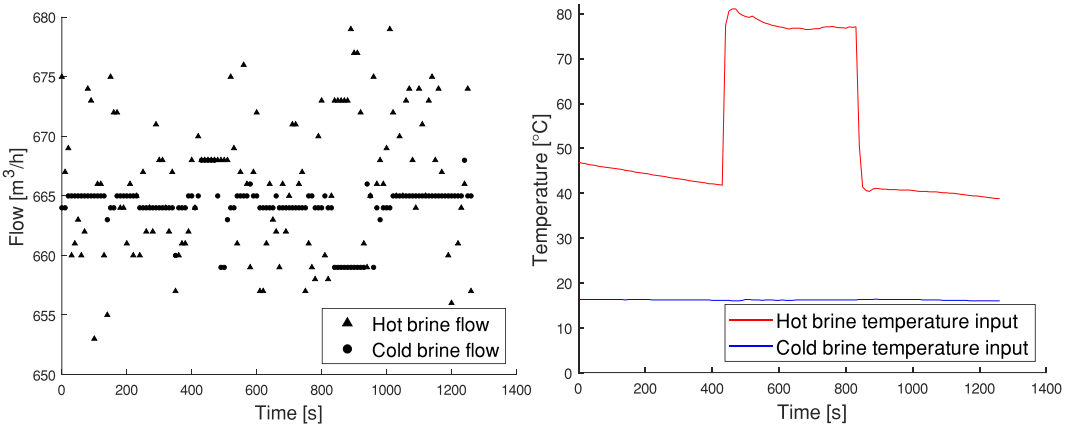

Fig. A2. Test flow and temperatures of test 2.

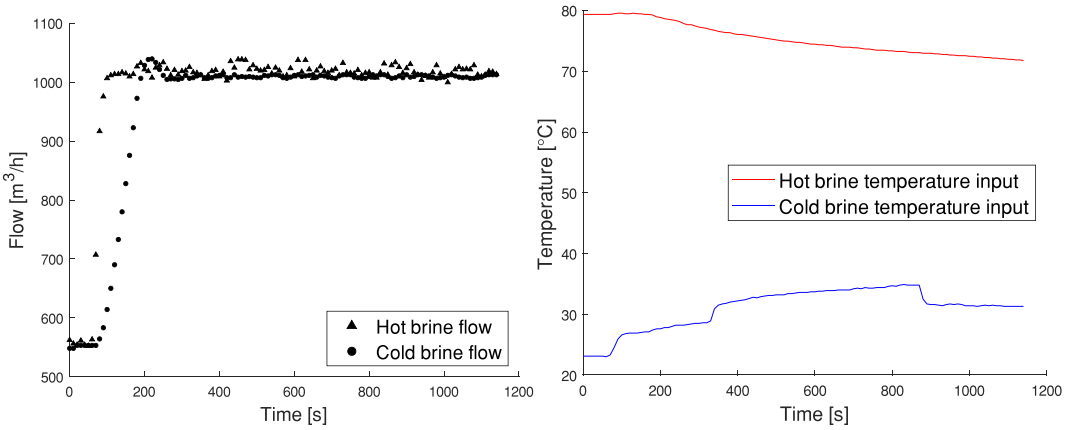

Fig. A3. Test flow and temperatures of test 3.

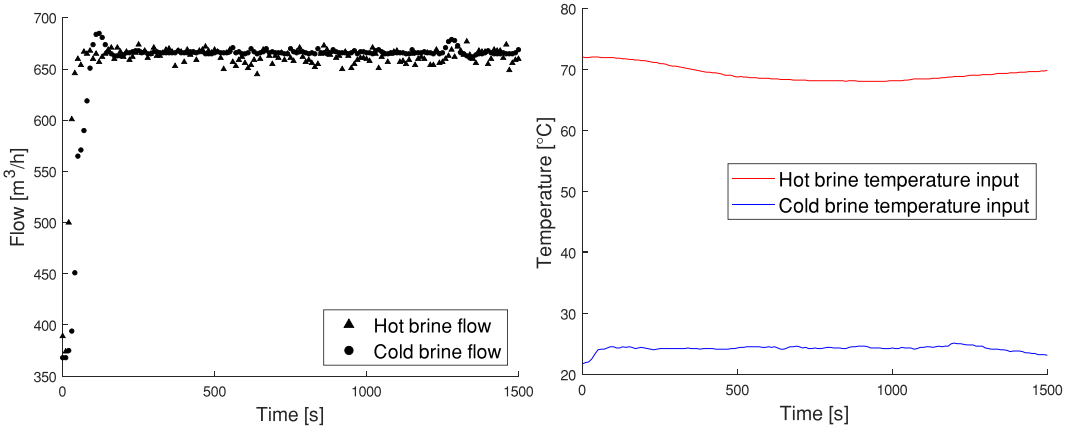

Fig. A4. Test flow and temperatures of test 4.

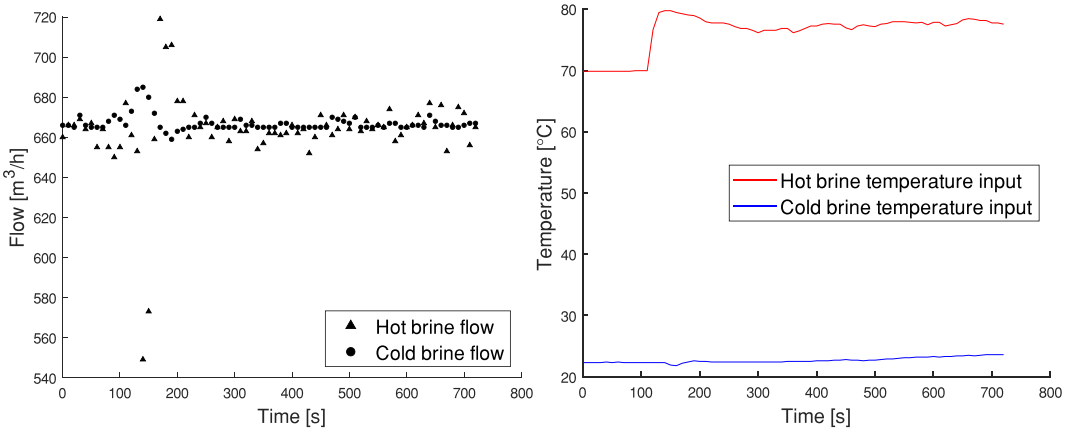

Fig. A5. Test flow and temperatures of test 5.

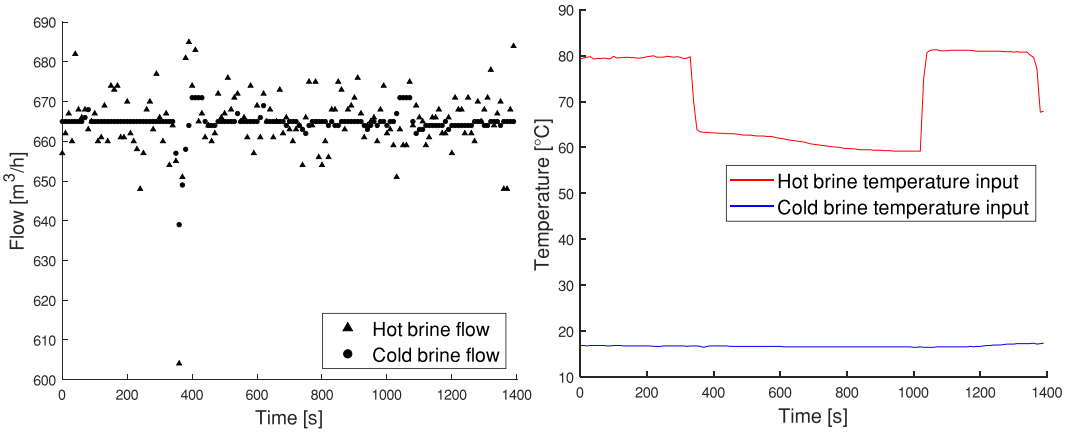

Fig. A6. Test flow and temperatures of test 6.

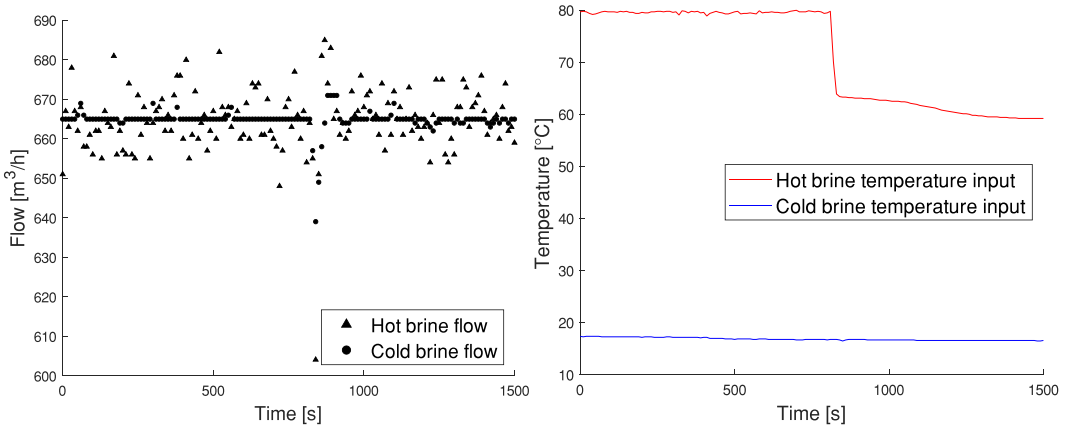

Fig. A7. Test flow and temperatures of test 7.

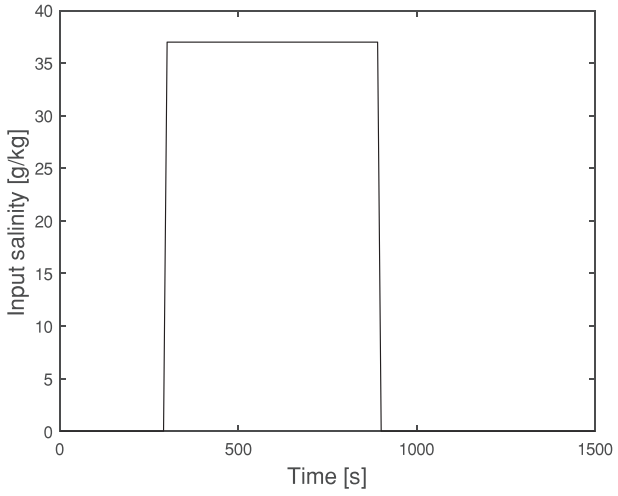

Fig. A8. Test input salinity of test 7 on the left.

References

[1] WWAP (UNESCO World Water Assessment Programme), The United Nations World Water Development Report 2019: Leaving No One Behind, UNESCO, Paris, 2019.

[2] I. Hitsov, L. Eykens, W. De Schepper, K. De Sitter, C. Dotremont, I. Nopens, Full-scale direct contact membrane distillation (DCMD) model including membrane compaction effects, J. Membr. Sci. 524 (2017) 245–256, https://doi.org/10.1016/j.memsci.2016.11.044.

[3] A. Alkhudhiri, N. Darwish, N. Hilal, Membrane distillation: a comprehensive review, Desalination. 287 (2012) 2–18, https://doi.org/10.1016/j.desal.2011.08.027.

[4] J.A. Andrés-Mañas, A. Ruiz-Aguirre, F.G. Acién, G. Zaragoza, Performance increase of membrane distillation pilot scale modules operating in vacuum-enhanced air-gap configuration, Desalination. 475 (2020) 114202, https://doi.org/10.1016/j.desal.2019.114202.

[5] W.G. Shim, K. He, S. Gray, I.S. Moon, Solar energy assisted direct contact membrane distillation (DCMD) process for seawater desalination, Sep. Purif. Technol. 143 (2015) 94–104, https://doi.org/10.1016/j.seppur.2015.01.028.
[6] M.R. Qtaishat, F. Banat, Desalination by solar powered membrane distillation systems, Desalination. 308 (2013) 186–197, https://doi.org/10.1016/j.desal.2012.01.021.
[7] G. Zaragoza, J.A. Andrés-Mañas, A. Ruiz-Aguirre, Commercial scale membrane distillation for solar desalination, NPJ Clean Water. 1 (2018) 1–6, https://doi.org/10.1038/s41545-018-0020-z.
[8] A. Ruiz-Aguirre, M.I. Polo-López, P. Fernández-Ibáñez, G. Zaragoza, Assessing the validity of solar membrane distillation for disinfection of contaminated water, Desalin. Water Treat. 55 (2015) 2792–2799, https://doi.org/10.1080/19443994.2014.946717.
[9] A. Ruiz-aguirre, D.-C. Alarcón-Padilla, G. Zaragoza, Productivity analysis of two spiral-wound membrane distillation prototypes coupled with solar energy, Desalin. Water Treat. 55 (2015) 2777–2785, https://doi.org/10.1080/19443994.2014.946711.
[10] A. Ruiz-Aguirre, J.A. Andrés-Mañas, J.M. Fernández-Sevilla, G. Zaragoza, Experimental characterization and optimization of multi-channel spiral wound air gap membrane distillation modules for seawater desalination, Sep. Purif. Technol. 205 (2018) 212–222, https://doi.org/10.1016/j.seppur.2018.05.044.
[11] H. Chang, G.B. Wang, Y.H. Chen, C.C. Li, C.L. Chang, Modeling and optimization of a solar driven membrane distillation desalination system, Renew. Energy 35 (2010) 2714–2722, https://doi.org/10.1016/j.renene.2010.04.020.
[12] K. Rahaoui, L.C. Ding, L.P. Tan, W. Mediouri, F. Mahmoudi, K. Nakoa, A. Akbarzadeh, Sustainable membrane distillation coupled with solar pond, Energy Procedia 110 (2017) 414–419, https://doi.org/10.1016/j.egypro.2017.03.162.
[13] K. Nakoa, K. Rahaoui, A. Date, A. Akbarzadeh, An experimental review on coupling of solar pond with membrane distillation, Sol. Energy 119 (2015) 319–331, https://doi.org/10.1016/j.solener.2015.06.010.
[14] F. Suárez, S.W. Tyler, A.E. Childress, A theoretical study of a direct contact membrane distillation system coupled to a salt-gradient solar pond for terminal lakes reclamation, Water Res. 44 (2010) 4601–4615, https://doi.org/10.1016/j.watres.2010.05.050.
[15] H. Chen, Z. Ye, W. Gao, A desalination plant with solar and wind energy, in: IOP Conf, Ser. Mater. Sci. Eng., 2013 https://doi.org/10.1088/1757-899X/52/7/072003.
[16] M. Gryta, The concentration of geothermal brines with iodine content by membrane distillation, Desalination. 325 (2013) 16–24, https://doi.org/10.1016/j.desal.2013.06.019.
[17] H. Chang, G.-B. Wang, Y.-H. Chen, C.-C. Li, C.-L. Chang, Modeling and optimization of a solar driven membrane distillation desalination system, Renew. Energy 35 (2010) 2714–2722, https://doi.org/10.1016/j.renene.2010.04.020.
[18] E. Ali, Dynamic analysis and modeling of direct contact membrane distillation for water desalination during startup using linear system theory, Chem. Eng. Process. Process Intensif. 136 (2019) 17–27, https://doi.org/10.1016/j.cep.2018.12.003.
[19] F. Eleiwi, N. Ghaffour, A.S. Alsaadi, L. Francis, T.M. Laleg-Kirati, Dynamic modeling and experimental validation for direct contact membrane distillation (DCMD) process, Desalination. 384 (2016) 1–11, https://doi.org/10.1016/j.desal.2016.01.004.
[20] A.M. Karam, A.S. Alsaadi, N. Ghaffour, T.M. Laleg-Kirati, Analysis of direct contact membrane distillation based on a lumped-parameter dynamic predictive model, Desalination. 402 (2017) 50–61, https://doi.org/10.1016/j.desal.2016.09.002.
[21] R. Porrazzo, A. Cipollina, M. Galluzzo, G. Micale, A neural network-based optimizing control system for a seawater-desalination solar-powered membrane distillation unit, Comput. Chem. Eng. 54 (2013) 79–96, https://doi.org/10.1016/j.compchemeng.2013.03.015.
[22] E. Ali, J. Saleh, J. Orfi, A. Najib, Developing and validating linear dynamic models for direct contact membrane distillation during start-up over wide operating conditions, Comput. Chem. Eng. 134 (2020). doi:https://doi.org/10.1016/j.compchemeng.2019.106678.
[23] E. Ali, J. Orfi, A. Najib, Developing and validating a dynamic model of water production by direct-contact membrane distillation, PLoS One 15 (2020) 1–24, https://doi.org/10.1371/journal.pone.0230207.
[24] M. Bindels, N. Brand, B. Nelemans, Modeling of semibatch air gap membrane distillation, Desalination. 430 (2018). doi:https://doi.org/10.1016/j.desal.2017.12.036.
[25] I. Hitsov, K. De Sitter, C. Dotremont, P. Cauwenberg, I. Nopens, Full-scale validated air gap membrane distillation (AGMD) model without calibration parameters, J. Membr. Sci. 533 (2017) 309–320, https://doi.org/10.1016/j.memsci.2017.04.002.
[26] I. Hitsov, T. Maere, K. De Sitter, C. Dotremont, I. Nopens, Modelling approaches in membrane distillation: a critical review, Sep. Purif. Technol. 142 (2015) 48–64, https://doi.org/10.1016/j.seppur.2014.12.026.
[27] A.S. Alsaadi, N. Ghaffour, J.D. Li, S. Gray, L. Francis, H. Maab, G.L. Amy, Modeling of air-gap membrane distillation process: a theoretical and experimental study, J. Membr. Sci. 445 (2013) 53–65, https://doi.org/10.1016/j.memsci.2013.05.049.
[28] J. Zhang, S. Gray, J. De Li, Modelling heat and mass transfers in DCMD using compressible membranes, J. Membr. Sci. 387–388 (2012) 7–16, https://doi.org/10.1016/j.memsci.2011.08.034.
[29] J. Swaminathan, H.W. Chung, D.M. Warsinger, J.H.L. V, Membrane distillation model based on heat exchanger theory and configuration comparison, Appl. Energy. 184 (2016) 491–505. doi:https://doi.org/10.1016/j.apenergy.2016.09.090.
[30] S. Burke, D. Ph, Computer Experiments : Space Filling Design and Gaussian Process Modeling, (2018). https://www.afit.edu/stat/statcoe_files/Computer Experiments-Space Filling Designs and Gaussian Process Modeling.pdf.
[31] V.R. Joseph, Space-filling designs for computer experiments: a review, Qual. Eng. 28 (2016) 28–35, https://doi.org/10.1080/08982112.2015.1100447.
[32] F. Wahl, F. Wahl, Measuring the quality of maximin space-filling designs, in: Special Issue on the Third Stu Hunter Research Conference Volume 28, Issue 1, 2016, pp. 28–35. https://www.tandfonline.com/doi/abs/10.1080/08982112.2015.1100447?journalCode=lqen20.
[33] V.R. Joseph, E. Gul, S. Ba, Maximum projection designs for computer experiments, Biometrika. 102 (2015) 371–380, https://doi.org/10.1093/biomet/asv002.
[34] The R Foundation, The R Project for Statistical Computing. https://www.r-project.org/, 2019.
[35] V.R. Joseph, E. Gul, S. Ba, MaxPro: Maximum Projection Designs, (2018). https://cran.r-project.org/web/packages/MaxPro/index.html (accessed April 6, 2019).
[36] M. Starzak, S. Peacock, Water activity coefficient in aqueous solutions of sucrose- a comprehensive data analysis, Zuckerindustrie.Sugar Ind. (1997) 380–387.
[37] R. Darros-Barbosa, M.O. Balaban, A.A. Teixeira, Temperature and concentration dependence of density of model liquid foods, Int. J. Food Prop. 6 (2003) 195–214, https://doi.org/10.1081/JFP-120017815.
[38] M. Asadi, Beet-sugar Handbook, Wiley, 2005, https://doi.org/10.1002/9780471790990.
[39] F. Chenlo, R. Moreira, G. Pereira, A. Ampudia, Viscosities of aqueous solutions of sucrose and sodium chloride of interest in osmotic dehydration processes, J. Food Eng. 54 (2002) 347–352, https://doi.org/10.1016/S0260-8774(01)00221-7.
[40] M. Werner, A. Baars, F. Werner, C. Eder, A. Delgado, Thermal conductivity of aqueous sugar solutions under high pressure, Int. J. Thermophys. 28 (2007) 1161–1180, https://doi.org/10.1007/s10765-007-0221-z.
[41] R.H. Myers, D.C. Montgomery, C.M. Anderson-Cook, Response Surface Methodology: Process and Product Optimization Using Designed Experiments, 2016.
[42] D.C. Montgomery, E.A. Peck, G.G. Vining, Introduction to Linear Regression Analysis. (2012), https://doi.org/10.2307/2348362.